Published in final edited form as:
Comp Biochem Physiol C Toxicol Pharmacol. 2012 January ; 155(1): 128–135. doi:10.1016/j.cbpc.2011.03.006.

Identification of Differentially Expressed Thyroid Hormone Responsive Genes from the Brain of the Mexican Axolotl (*Ambystoma mexicanum*) ✧

P Huggins[1,a], **CK Johnson**[1,b], **A Schoergendorfer**[1,a], **S Putta**[b], **AC Bathke**[a], **AJ Stromberg**[a], and **SR Voss**[b,*]

P Huggins: peter.huggins@uky.edu; CK Johnson: carlena.johnson@uky.edu; A Schoergendorfer: angela.sch@uky.edu; S Putta: sputt2@email.uky.edu; AJ Stromberg: astro11@email.uky.edu

[a] Department of Statistics, University of Kentucky, Lexington, KY 40506, USA

[b] Department of Biology, University of Kentucky, Lexington, KY 40506, USA

Abstract

The Mexican axolotl (*Ambystoma mexicanum*) presents an excellent model to investigate mechanisms of brain development that are conserved among vertebrates. In particular, metamorphic changes of the brain can be induced in free-living aquatic juveniles and adults by simply adding thyroid hormone (T4) to rearing water. Whole brains were sampled from juvenile *A. mexicanum* that were exposed to 0, 8, and 18 days of 50 nM T4, and these were used to isolate RNA and make normalized cDNA libraries for 454 DNA sequencing. A total of 1,875,732 high quality cDNA reads were assembled with existing ESTs to obtain 5,884 new contigs for human RefSeq protein models, and to develop a custom Affymetrix gene expression array (Amby_002) with approximately 20,000 probe sets. The Amby_002 array was used to identify 303 transcripts that differed statistically ($p < 0.05$, fold change > 1.5) as a function of days of T4 treatment. Further statistical analyses showed that Amby_002 performed concordantly in comparison to an existing, small format expression array. This study introduces a new *A. mexicanum* microarray resource for the community and the first lists of T4-responsive genes from the brain of a salamander amphibian.

1. Introduction

Thyroid hormone (TH) is essential for normal development of the mammalian brain. Maternal, fetal, and neonatal TH levels are closely regulated in temporal and spatial contexts to affect proper cell migration, proliferation, and differentiation, and to orchestrate synaptogenesis and myelination of neurons (Anderson et al., 2003; Koibuchi, 2008; Patel et al., 2011). Later in life, thyroid hormone affects the activity of neuroendocrine axes that regulate reproduction, appetite, behavior, stress response, and longevity (Ooka and Shinkai, 1986; Shi et al., 1994; Gussekloo et al., 2004; Kong et al., 2004; Brambilla et al., 2006; Leggio et al., 2008; Duval et al., 2010; Krassas et al., 2010). That so many fundamental biological processes are associated with the action of a single molecule reflects in part the molecular mechanisms through which TH operates. It has been known for some time that

✧This paper is based on a presentation given at the *5th Aquatic Annual Models of Human Disease* conference: hosted by Oregon State University and Texas State University-San Marcos, and convened at Corvallis, OR, USA September 20-22, 2010.

* Communicating author: Randal Voss: srvoss@uky.edu, Tel: 859-257-9888; Fax: 859-257-1717.

[1] Co-First Authors

✧This paper is based on a presentation given at the *5th Aquatic Annual Models of Human Disease* conference: hosted by Oregon State University and Texas State University-San Marcos, and convened at Corvallis, OR, USA September 20-22, 2010.

TH interacts with nuclear receptors (TRα or TRβ) and cofactors to regulate transcription directly (Openheimer et al., 1974; Samuels et al., 1974; Sap et al., 1986; Weinberger et al., 1986), and recent studies are beginning to use unbiased approaches to identify TH-regulated genes in the brain (e.g. Royland et al., 2008; Das et al., 2009). Much less is known about the way TH signals via “non-genomic” mechanisms, including membrane receptors, transporter molecules, and cytoplasmic receptors that elicit changes in cells through signaling pathways (Caria et al., 2009; reviewed by Davis et al., 2008; Furuya et al., 2009; Cheng et al., 2010). Identification of additional TH-regulated genes and molecular mechanisms will require continued studies of traditional models and development of new models.

Many mechanisms that are associated with TH synthesis, activation, and transcriptional regulation are evolutionarily conserved among vertebrates, and these presumably function during homologous stages of development (Tata, 1993; 2006). Thus, it is possible to investigate mechanisms of mammalian brain development in more experimentally tractable organisms with free-living embryonic and juvenile phases. Anuran amphibians in particular have been extensively studied because it is straightforward to induce metamorphosis in tadpoles with TH and investigate how TH affects developmental changes in vivo through interactions with TRs, accessory co-factors, and changes in chromatin state (e.g. Shi, 2000; Das et al., 2010; Bilesimo et al., 2011). TH levels increase precipitously during anuran metamorphosis to regulate the development of adult tissue and organ systems from pre-existing larval structures and progenitor cell populations. In humans, TH levels similarly increase as the brain matures during the perinatal stage of early development (Brown et al., 2005). Thus, the study of anuran metamorphosis may identify TH-dependent mechanisms that are critical for normal human brain development. However, there are limitations in using anuran models to study the actions of TH. Although it is straightforward to administer TH, dosing regimes are generally administered at developmental stages when TH levels are relatively low in tadpoles. Because genes maybe differentially responsive to TH as a function of age, precocious administration of TH may activate or repress genes that are not typical of normal development and metamorphosis. Also, when tadpoles of spontaneously metamorphosing anurans are exposed to TH, they are already developing toward a metamorphic endpoint; thus anurans do not provide a true negative control for evaluating TH signaling.

The Mexican axolotl (*Ambystoma mexicanum*) provides an alternative amphibian model to investigate TH signaling (Page et al., 2007; 2008; 2009). While many amphibians undergo an obligate metamorphosis, *A. mexicanum* juveniles fail to produce enough TH to induce metamorphosis (Kuhn, 1989; Galton 1991). As a result, *A. mexicanum* retain juvenile traits into the adult stage of life, an adaptation that has been termed paedomorphosis. Importantly, metamorphosis can be induced in *A. mexicanum* by simply adding the thyroxine form of TH (T4) to the water (Page and Voss, 2009). Thus, developmental events can be induced within the context of a natural, hypothyroid condition at juvenile or adult stages of life. In *A. mexicanum*, paedomorphosis is associated with an unidentified genetic factor that affects developmental timing, response to T4, and hypothalamic-pituitary-thyroid function (Voss and Smith 2005; Galton 1991; Rosenkilde, 1996; Kuhn 2005).

In previous studies, we used microarray analysis to show that metamorphosis is precisely and reliably induced in *A. mexicanum* using 5 or 50 nM T4 (Page et al., 2007; Page et al., 2008). We also reported an integrative model of epidermal gene expression and whole-animal anatomical metamorphosis (Page et al., 2009). Here, we report on a study that used highly parallel 454 DNA sequencing to discover genes from the *A. mexicanum* brain. The resulting sequence reads were assembled with pre-existing ESTs from Sal-Site (www.ambystoma.org) to design a 2nd generation custom Affymetrix expression array (Amby_002). This new microarray platform was then used to identify genes that are

differentially expressed in the *A. mexicanum* brain after treatment with T4. Our study enhances the *A. mexicanum* model by providing a new microarray resource and new EST contigs that increase the total number of *Ambystoma*-human non-redundant orthologous sequences to >15,000. Also, our study provides the first lists of T4 -responsive genes from a salamander amphibian, including genes that are predicted to function in neural developmental and physiological processes within the brain.

2. Materials and methods

2.1 Animals and Tissue Sampling

Nine *A. mexicanum* juvenile siblings were obtained from the *Ambystoma* Genetic Stock Center at the University of Kentucky and reared under the same laboratory conditions to approximately 130 days post hatching. At this age, individuals are immature with respect to gonad maturation and have surpassed the time that metamorphosis typically occurs in related species. Three individuals were anesthetized in 0.02% benzocaine and the brains and pituitaries of each were removed, flash frozen in ethanol and liquid nitrogen, and stored separately at -80 C until the time of RNA isolation. The other 6 individuals were reared individually in a 50 nM T4 (Sigma, St. Louis, MO; T2376) prepared according to the method of Page and Voss (2009). When juveniles are reared in 50 nM T4, morphological metamorphosis initiates approximately 8 days after treatment, morphology rapidly changes between days 15-20, and metamorphosis is completed after approximately 28-32 days (Page et al., 2009). We observed early signs of anatomical metamorphosis at Day 8 and changes indicative of metamorphic climax at D18. After 8 and 18 days of treatment, 3 individuals were sacrificed and brain/pituitary tissue was removed and stored as described above. This sampling design yielded three replicates of brain tissue for three groups: no T4 (D0), early metamorphosis (D8), and metamorphic climax (D18). Animal care and use was carried out under University of Kentucky IACUC protocols #01087L2006 and #00907L2005.

2.2 RNA isolation and 454 DNA sequencing

Total RNA was isolated using TRIzol (Invitrogen, Carlsbad, CA) and RNA samples were further purified using Qiagen RNeasy mini-columns. RNA samples were quantified using a NanoDrop ND-1000 and Agilent BioAnalyzer. RNA from one replicate of each treatment was used to make cDNA libraries for 454 DNA sequencing. We refer to these as 454_D0, 454_D8, and 454_D18. cDNA libraries were generated using standard methods of MINT cDNA synthesis and TRIMMER cDNA normalization kits from EVROGEN, Inc; sequences were size-selected according to manufacturer's instructions. cDNAs were sequenced by the University of Iowa Biology Department Sequencing Core using the Genome Sequencer FLX System with Titanium Chemistry (Roche Applied Science, Indianapolis, IN). SeqClean (http://www.tigr.org/tdb/tgi/software) was used for vector/poor quality trimming, bacterial contaminant screening, and identification of *A. mexicanum* mitochondrial DNA and rDNA sequences. Retained sequences were assembled using Newbler (Version 2.0.01.14) from 454 Life Sciences. Contigs (including singletons) were searched using BLAST algorithms against the *Ambystoma* ESTdb at Sal-Site (Smith et al., 2005), and NCBI protein and nucleotide databases. Queries that returned significant BLAST hits were assigned the gene identifier of the best-matching subject sequence. 454 DNA sequence reads were assembled with previous EST data and the overall assembly is available at Sal-Site. Assembled contigs were submitted to Affymetrix to design approximately 20,000 perfect-match probe sets for a custom gene expression array: Amby_002 (Part Number 520748).

2.3 Microarray Analysis

Genome-level expression profiling was conducted using Amby_002 and Amby_001, a small format array (~4500 probe sets) that was designed in 2005 from approximately 60,000 ESTs

(Smith et al., 2005). Amby_001 has been used to quantify gene expression in several experiments (Page et al., 2007, 2008; Monaghan et al., 2007, 2009; Cotter et al 2008), including an experiment that examined brain tissues from *A. mexicanum* and *A. t. tigrinum* (Page et al., 2010). RNA from all 9 of the brain samples was labeled, hybridized to separate Amby_002 arrays, and scanned by the University of Kentucky Microarray Core Facility according to standard Affymetrix protocols. We also hybridized the three D0 and D18 replicates to six Amby_001 arrays to investigate concordance and discordance between the Affy platforms. Background correction, normalization, and expression summaries were obtained using the robust multi-array average (RMA) algorithm (Irizarry et al. 2003).

2.4 Identification of differentially expressed genes (DEGs) using microarrays

The expression data from Amby_002 were examined using standard *F-tests* to identify genes that were differentially expressed as a function of T4 treatment. Then *t-tests* were applied to this list of DEGs to identify the direction of gene expression change between the D0, D8, and D18 time points. For example, between D0 and D8 an expression change can be described as up, down, or unchanged. See Supplementary File 1 for details on how F-tests and t-tests were performed. All statistical analyses were performed using SAS 9.2 (SAS Institute Inc, Cary, NC, USA) and R 2.11.0 (www.r-project.org).

2.5 Statistical comparison of microarray platforms

We applied several statistical techniques to compare expression values between Amby_001 and Amby_002 for the D0 and D18 groups. We restricted attention to 2601 comparable probe set pairs, i.e. pairs of probe sets that were designed to target the same gene. Probability values (p-values) for differential expression between groups D0 and D18 were computed for each microarray platform, using t-tests applied to RMA normalized expression values. We computed the Spearman correlation among p-values for Amby_001 and Amby_002, as well as correlation among log fold change expression values.

We then estimated the percentage of discordant comparable probe set pairs; i.e. comparable probe set pairs that exhibited detectable measurement differences between groups D0 and D18. To do this we computed p-values for the treatment × platform interaction in a linear model for gene expression. In order to avoid underestimating discordant probe set pairs, we used a highly sensitive counting approach that analyzed the interaction terms' overall p-value histogram, rather than testing individual p-values. A more in depth treatment of these statistical methods is provided in Supplemental File 1.

2.6 Identification of statistically enriched biological processes

To identify biological processes that were statistically enriched in lists of DEGs, we conducted enrichment analyses using PANTHER (Thomas et al., 2003). For all analyses, the probe sets on Amby_001 and Amby_002 that showed significant sequence identity to vertebrate NCBI RefSeq proteins were used to generate expected values (i.e., the background). Only gene ontology terms with two or more supporting genes were reported and the significance threshold was set to 0.05. The lists of significant GO terms were manually inspected to remove redundant terms.

3. Results

3.1 Identification of genes from A. mexicanum brain using 454 DNA sequencing

To generate new ESTs from *A. mexcianum* brain, cDNAs were synthesized for three brain samples: a brain isolated from a 133 day old individual (D0_454), and brains isolated from 141 and 151 day old individuals that had been reared for 8 and 18 days in 50 nM T4, respectively (D8_454; D18_454). Overall 2.06×10^6 reads were generated and this yielded

approximately 584,000-699,000 high-quality sequence reads for each sample, with an average of 374 base pairs in length (Table 1). Typically, 30-50% of transcripts correspond to mitochondrial and ribosomal sequences when non-normalized cDNA libraries are sequenced (Putta et al. 2004; Monaghan et al., 2009). Here, application of a cDNA normalization procedure before sequencing efficiently reduced mitochondrial and ribosomal sequence reads to < 3%. Assembly of all high-quality cDNA reads yielded 915,442 unique sequences. These sequences were assembled with previous EST contigs from Monaghan et al. (2009) to produce 127,484 contigs each containing at least two overlapping sequences. All contigs and singletons were searched against NCBI databases to identify significant similarity matches that would suggest presumptive gene identities. *A. mexicanum* contigs and singletons yielded 62,100 significant hits to sequences in the human RefSeq database (BLASTx, $e < 1 \times 10\text{-}7$), including 15,384 unique human genes. Assembly of the new brain-derived sequence reads with existing EST contigs from the Ambystoma EST database increased the number of non-redundant human-*A. mexicanum* orthologous sequences by 5,884, and these annotated to 129 and 127 different biological process and PANTHER pathway annotations, respectively. The highest numbers of genes annotated to general cellular (N=2110) and metabolic processes (N=2457) including cell communication (N=1607), signal transduction (N=1520), nucleobase, nucleoside, nucleotide and nucleic acid metabolic process (N=1174), and transport (N=1016) (Table 1). The annotations for Panther biological pathways show that the 454 DNA sequencing approach was highly successful in discovering new genes associated with neural developmental and physiological processes (Table 2). Genes for developmental signaling pathways were identified, including Wnt (N=119), Cadherin (N=59), PDGF (N=53), EGF (N=49), TGF-B (N=42), Endothelin (N=41), FGF (N=40), p53 (N=33), VEGF (N=32), PI3 kinase (N=31), IGF (N=30), Notch (N=15), and Hedgehog (N=10). Also, genes for a diverse group of neural receptor signaling pathways were identified, including those involving metabotrophic glutamate receptors (N=91), serotonin (5HT1-4) receptors (N=77), muscarinic acetylcholine receptors 1-4 (N=61), nicotinic acetylcholine receptors (N=39), GABA-B receptor 2 (N=17), and ionotropic glutamate receptors (N=38). Finally, genes were identified for thyrotrophin (N=33) and corticotrophin releasing factor signaling pathways (N=12), the later of which functions in amphibians to regulate the release of thyroid hormone and glucocorticoids during metamorphosis.

3.2 Identification of differentially expressed genes using the Amby_002 GeneChip

The contigs that were assembled using brain 454 DNA reads and existing Sal-Site (www.ambystoma.org) ESTs were used to develop a custom Affymetrix expression array (Amby_002) with approximately 20,000 perfect-match probe sets. The Amby_002 microarray was used to estimate brain mRNA abundances from *A. mexicanum* juveniles that received 0, 8, and 18 days of 50 nM thyroid hormone (T4) treatment. Using statistical and fold change thresholds ($p < 0.05$ and fold change > 1.5 for at least one contrast), a total of 303 probe sets yielded significantly different hybridization intensities (transcript abundances) among the three time points that were compared (Supplemental File 2). The list of 303 DEGs included 16 redundant probe set pairs and 1 probe set trio that were designed to target the same reference gene. In all 17 of these cases, redundant probe sets registered similar estimates of transcript abundance and the same directional change among the time points. After accounting for probe set redundancy, the list of differentially expressed genes (DEGs) includes 218 with predicted gene names and 67 that correspond to unknown transcripts.

PANTHER databases and tools were used to annotate gene ontologies to the 218 DEGs and identify enriched biological processes and pathways. First, the frequency of ontology terms for the 218 DEGs was compared to a reference list (N=11353) compiled for all annotatable probe sets on Amby_002. This yielded 11 enriched biological process ontologies (Table 4)

and 7 PANTHER pathways at $P < 0.05$: cholesterol biosynthesis (N=4), glycolysis/fructose galactose metabolism (N=3), GABA-B receptor II signaling (N=4), Notch signaling pathway (N=4); formyltetrahydroformate biosynthesis (N=2), heterotrimeric G-protein signaling pathway-Gi alpha and Gs alpha (N=6), and DNA replication (N=2). The overall DEG list was then partitioned to associate biological process ontologies with groups of genes that showed similar temporal changes in transcript abundance. For example, transcripts for 71 DEGs increased significantly between D0 and D8, while 40 DEGs decreased significantly during this time interval (Table 4). The DEGs that increased in abundance between D0 and D8 annotated to processes suggesting a role in cell cycle regulation. Several of these genes function to promote a cell's progression or arrest through the cell cycle (*ccna2*, *cdk7*, *ccnc*, *ccncb3*, *tbrg4*, *cdnk1c*, *revl3*). In comparison to the genes that increased during D0-D8, only 1 significant biological process (anion transport: *chrne*, *chrng*) was identified for genes that decreased in abundance between D0-D8. The majority of these genes mapped to different biological processes, although two genes (*hes5*, *hes6*) mapped to the Notch signaling pathway.

More biological process terms were identified for DEGs identified for the D8-D18 time period (Table 4). Eight of 11 biological process ontology terms that were identified using all genes were also identified for the group of genes that decreased in abundance between D8 and D18, and many of these were associated with metabolic process terms. Also, genes that encode hemoglobin subunits (*hbe*, *hba2*) expressed during fetal stages of development in mammals were observed to decrease in abundance, as did growth hormone (*gh1*) and *dnmt1*, *a* methyltransferase that establishes and maintains tissue specific patterns of DNA methylation. Sixteen genes that are predicted to function in neurological system processes increased in abundance (Table 5), as did genes associated with lipid (N=11) and vitamin (N=5) metabolic processes. The neurological system process genes encode proteins that function in multiple processes, including steroid and peptide hormone binding (*nr3c2*, *hcrtr2*, *nrip1*), synaptogenesis (*nlgn4x*), synaptic transmission (*ehd3*, *rasl11a*, *gda*), and neural development and patterning (*tulp3*).

3.3 Statistical comparison of microarray platforms

The same D0 and D18 samples that were hybridized to Amby_002 arrays were also hybridized to Amby_001, a first generation custom expression array with 3,729 gene-annotated probe sets. Mean D0 and D18 RMA log expression values were calculated for 2601 probe set pairs that presumably targeted the same gene on each array, and then the difference in mean expression (i.e. the log fold change) was compared between microarray platforms. Amby_001 and Amby_002 exhibited a Spearman correlation of $r_s = 0.76$ for the complete list of probe sets. When measuring differentially expressed transcripts, the two platforms exhibited very strong statistical agreement; the correlation of log fold change increased to $r_s = 0.94$ for 281 probe set pairs whose fold change was significant at $p < 0.1$ on both Amby_001 and Amby_002 (Figure 1; Supplemental File 3). We note that the strong correlation between microarray platforms is also robust to fold-change cutoff. For example, the correlation between platforms was at least $r_s = 0.93$ for fold changes as small as 1.2 (Figure 2). As a further indication of the strong agreement between platforms, the estimated percentage of discordant probe set pairs between platforms was only 5.3%.

4. Discussion

Amphibians provide excellent models to investigate the effects of thyroid hormone on development. An important advantage in using *A. mexicanum* over anuran models is the ability to reliably stimulate the onset of metamorphosis in juveniles or adults. This study is the first to use *A. mexicanum* to identify genes that are expressed differentially in the brain after inducing metamorphosis with T4. Below, we discuss the approach taken to identify

new brain transcripts and measure their abundance during metamorphosis, and then discuss the gene expression results.

4.1. 454 DNA sequencing and gene discovery

Our study shows that 454 DNA sequencing can be used to efficiently discover genes from specific tissues and design microarray resources to reliably and precisely quantify temporal changes in gene expression. Over 5,800 new contigs that match human RefSeq proteins were assembled from 454 DNA reads that were sampled from three normalized cDNA *A. mexicanum* brain libraries. The normalization procedure greatly reduced the representation of mitochondrial and ribosomal sequences that are synthesized when using an oligo-dT priming approach to generate cDNA from RNA (Monaghan et al., 2009). This increased the discovery process for brain-associated transcripts. It is also important to note that the 454 DNA sequence generated from this study provided additional sequencing depth and length for existing EST contigs at Sal-Site. This allowed us to develop a new community resource – the Amby_002 expression array. We showed statistically that the new Amby_002 array provides estimates of gene expression that are concordant with the earlier Amby_001 array, however Amby_002 has approximately 5× more probe sets than Amby_001 and thus allows greater resolution of gene expression. Using Amby_002, we identified 303 differentially expressed brain transcripts that correspond to 218 *A. mexicanum*-human orthologous protein-coding sequences. Of the 218, 131 corresponded to probe sets that are unique to the Amby_002 array and are not represented on Amby_001. Thus, 60% of the DEGs that were identified in this study would not have been identified using the Amby_001 array.

4.2 TH-induced genes in the A. mexicanum brain

The DEGs identified in this study show that TH-induced brain metamorphosis in *A. mexicanum* is associated with a diversity of biological processes. These include genes that annotated to metabolic, cell cycle and signaling, and neurological systems ontologies. Thyroid hormone has long been associated with cellular macromolecular biosynthesis in both mammals and amphibians (Tata, 1993). As amphibian larvae mature, increasing levels of TH alter cellular metabolic processes to meet the energetic demands of metamorphosis. Three of the 7 significantly enriched PANTHER pathway terms identified from the complete list of DEGs annotated to cellular metabolic ontologies: glycolysis/fructose galactose metabolism (*aldob, aldoc, hk2*), formyltetrahydroformate biosynthesis (*mthfd1, tyms*), and cholesterol biosynthesis (*fdps, hmgcs1, lss, pmvk*). Other presumably up-regulated DEGs that were associated with metabolism but not identified by PANTHER include *pea15* (autophagy and glucose metabolism), *cyp2a13* (cholesterol/lipid metabolism in endoplasmic reticulum), *cpt1a* (fatty acid oxidation in mitochondria), *pprc1* (activator of mitochondrial biogenesis), and *cycs* (electron transport in mitochondria). We note that TH-induced metabolic changes derive from changes in chromatin (*dotl1, dnmt1*), transcription (*gtf2ird2b, tcea2*), translation (*eif4e2, etf1, mars, nars2, trmt12*), and transport (*rhot1, tspo, dirc2*), and genes associated with these fundamental cellular processes were also identified.

With respect to cell cycle and signaling ontology terms, several genes were identified that encode proteins for regulation of cell cycle progression (*ccna2, cdk7, ccnc, ccncb3, tbrg4, revl3*) and arrest (*cdnk1c).* Although *usp16* was not associated with the cell cycle ontology by PANTHER, this gene is thyroid hormone responsive in mammalian liver and associated with histone H2A deubiquitination and cell cycle progression (Pihlajamäki et al., 2009). Because the protein products of cell cycle genes are generally regulated post transcriptionally, their functional significance is unclear. However, it is well established that TH regulates neuronal and glial cell proliferation, migration, and maturation during early mammalian development (Anderson et al., 2003; Koibuchi, 2008; Patel et al., 2011). Genes that function to regulate such processes likely are members of major signaling pathways and

this study identified DEGs belonging to MAPK (*mapkapk3*), Hedgehog (*tulp3*), Wnt (*dkk3*), FGF (*fgfbp1*), integrin (*arf6, crk, col6a3*), endothelin (*adcy2, adcy8*, and *prkx*), Notch (*Hes5, Hes6, lfng, Notch1)*, and heterotrimeric G-protein signaling pathways (*adcy2, adcy8, adora1, kcnj3, htr5a1, prkx*). Both *adcy2* and *adcy8* increased in abundance in response to TH; in mammals, the expression of adenylyl cyclases is developmentally regulated and associated with synaptic plasticity, behavior, and learning (Sanabra and Mengod, 2011). The Notch signaling pathway functions to regulate neural development by specifying cell proliferation and differentiation. All 4 Notch-pathway genes showed decreasing transcript abundances, a pattern suggestive of cell differentiation (Gaiano and Fishell, 2002). Future studies that localize mRNAs to specific cell types by *in situ* hybridization are needed to determine how these signaling pathways function to remodel existing neural networks and stimulate neurogenesis from progenitor cell populations.

The overall list of 218 DEGs contained 30 genes that annotated to the neural systems ontology. Sixteen of these genes were up regulated between D8-D18, and 4 of these are highlighted here: (1) *hcrtr2*, a cell surface receptor that binds hypothalamic peptides (orexin A and B) that regulate appetite and other behaviors (Wong et al., 2011); (2) *nr3c2*, a transcription factor that binds glucocorticoids and whose functions are associated with stress and aging (De Kloet et al., 1998); (3) *tulp3*, a heterotrimeric-G-protein-responsive intracellular signaling factor that functions in neural development and patterning (Cameron et al., 2003); and (4) *nlgn4x* which functions in synaptogenesis and is associated with autism (Bolliger et al., 2001).

4.3 Relationship of TH-induced genes to genes expressed during natural metamorphosis

A previous microarray study using Amby_001 compared the brain gene expression programs of chronologically matched larvae of *A. mexicanum* and *A. tigrinum tigrinum*, before and during the process of metamorphosis in the latter species (Page et al., 2010). In *A. t. tigrinum*, thyroid hormone increases during larval development (Norman et al., 1987) and this is thought to initiate metamorphosis through thyroid hormone receptors, as has been shown in anurans (Das et al., 2010). Hundreds of transcripts were observed to show the same temporal patterns of change between *A. t. tigrinum* and *A. mexicanum*, including genes associated with neural development and maturation. Thus, some aspects of brain development and function are conserved regardless of whether a larva is developing toward a metamorphic or paedomorphic outcome. However, many genes were expressed differently between the species and more profoundly so at the time *A. t. tigrinum* larvae underwent metamorphosis. These latter genes were interpreted as comprising a metamorphic transcriptional program, presumably induced directly or indirectly by increasing TH levels during development. A few of these presumptive metamorphic response genes were observed to show the same pattern of increase (*ccdc43, hmga1, glul, dnajb13, rpe65, gpx1, cyp2a13, nr3c2, cartpt, dkk3*) or decrease (*tyms, dnmt1, ptx3, prim1, hbe1, hba2, smc4, s100a2, kiff22, pbk*) in transcript abundance that was observed in this study. This validates these genes as TH-responsive and suggests that TH-response genes have been maintained in the paedomorphic *A. mexicanum* lineage since divergence from a common metamorphic ancestor (Shaffer and Voss, 1996). However, > 85% of the genes identified as uniquely expressed in *A. t. tigrinum* were not identified as differentially expressed in this study. This may reflect differences in experimental design and statistical approaches between the studies, and the possibility that TH-response varies among related species and at different times during ontogeny. Page et. al. (2010) characterized transcriptional responses when metamorphosis normally occurs in *A. t. tigrinum* (~50-90 days), while this study induced metamorphosis in 139 day old *A. mexicanum* juveniles. It is possible that transcriptional patterns change in response to TH as the brain matures; unfortunately, we did not evaluate control samples (i.e. no thyroid hormone) from 147 (D8) and 157 (D18) day old *A.*

mexicanum to test for this possibility. Another possibility is that transcription may be phenomenological with regard to TH treatment, although *A. mexicanum* show reproducible patterns of epidermal transcription across an order of magnitude range of TH treatment (Page et. al., 2008; 5-50 nM). Further studies are needed to investigate the transcriptional response to TH at different juvenile and adult stages of *A. mexicanum* development.

5. Conclusion

Amphibian metamorphosis provides an excellent model to study TH-responsive periods of development that are homologous among vertebrates. This study introduces a new *A. mexicanum* microarray resource for the community and the first lists of T4-responsive genes from the brain of a salamander amphibian. The Mexican axolotl (*A. mexicanum*) is an unusual, hypothyroidic salamander that is available from genetically homogenous laboratory stocks maintained at University of Kentucky. It will be important in future studies to detail transcriptional changes over narrower time intervals during metamorphosis, as this is a very dynamic process. Also, it will be important to determine how TH-induced transcriptional changes vary across species and ontogeny.

Supplementary Material

Refer to Web version on PubMed Central for supplementary material.

Acknowledgments

We thank Robert Page and Meredith Boley for inducing metamorphosis in the *A. mexicanum* juveniles that were used in this experiment and for collecting brain tissues. The research was supported by grant R24-RR016344 and the National Center for Research Resources (NCRR), a component of the National Institutes of Health (NIH). The project also used resources developed under Multidisciplinary University Research Initiative grant (W911NF-09-1-0305) from the Army Research Office, and resources from the *Ambystoma* Genetic Stock Center, which is funded by grant DBI-0951484 from the National Science Foundation. The contents of this paper are solely the responsibility of the authors and do not necessarily represent the official views of NCRR, NIH, ARO, or NSF.

References

Anderson GW, Schoonover CM, Jones SA. Control of thyroid hormone action in the developing rat brain. Thyroid. 2003; 13:1039–1056. [PubMed: 14651788]

Axelband FJD, Ferrao FM, Einicker-Lamas M. Nongenomic signaling pathways triggered by thyroid hormones and their metabolite 3-iodothyronaime on the cardiovascular system. J Cell Physiol. 2010; 226:21–28. [PubMed: 20658515]

Bernal J. Thyroid hormone receptors in brain development and function. Nat Clin Pract Endocrinol Metab. 2007; 3:249–259. [PubMed: 17315033]

Bilesimo P, Jolivet P, Alfama G, Buisine N, Le Mevel S, Havis E, Demeneix BA, Sachs LM. Specific histone lysine 4 methylation patterns define TR-binding capacity and differentiate direct T3 responses. Mol Endocrinol. 2011 Jan 14. Epub ahead of print.

Bolliger MF, Frei K, Winterhalter KH, Gloor SM. Identification of a novel neuroligin in humans which binds to PSD-95 and has a widespread expression. Biochem J. 2001; 356:581–8. [PubMed: 11368788]

Brambilla F, Santonastaso P, Caregaro L, Favaro A. Disorders of eating behavior: correlation between hypothalamo-pituitary-thyroid function and psychopathological aspects. Psychoneuroendocrinology. 2006; 31:131–136. [PubMed: 16112494]

Brown, RS.; Huang, SA.; Fisher, DA. The Maturation of Thyroid Function in the Perinatal Period and During Childhood. In: Braverman, LE.; Utiger, RD., editors. Werner and Ingbar's the Thyroid: a fundamental and clinical text. Lippincott Williams and Wilkins; Philadelphia: 2005. p. 1013-1028.

Cameron DA, Pennimpede T, Petkovich M. Tulp3 is a critical repressor of mouse hedgehog signaling. Dev Dyn. 2009; 238:1140–1149. [PubMed: 19334287]

Caria MA, Dratman MB, Kow LM, Mameli O, Pavlides C. Thyroid hormone action: nongenomic modulation of neuronal excitability in the hippocampus. J Neuroendocrinol. 2009; 21:98–107. [PubMed: 19076268]

Cheng SY, Leonard JL, Davis PJ. Molecular aspects of thyroid hormone actions. Endocr Revs. 2010; 31:139–70. [PubMed: 20051527]

Cotter JD, Storfer A, Page RB, Beachy CK, Voss SR. Transcriptional response of Mexican axolotls to *Ambystoma tigrinum* virus (ATV) infection. BMC Genomics. 2008; 9:493. [PubMed: 18937860]

Das B, Matsuda H, Fujimoto K, Sun G, Shi YB. Molecular and genetic studies suggest that thyroid hormone receptor is both necessary and sufficient to mediate the developmental effects of thyroid hormone. Gen Comp Endocrinol. 2010; 168:174–180. [PubMed: 20138179]

Das B, Heimeier RA, Buchholz DR, Shi YB. Identification of direct thyroid hormone response genes reveals the earliest gene regulation programs during frog metamorphosis. J Biol Chem. 2009; 284:34167–34178. [PubMed: 19801647]

Davis PJ, Leonard JL, Davis FB. Mechanisms of nongenomic actions of thyroid hormone. Front Neuroendocrinol. 2008; 29:211–218. [PubMed: 17983645]

De Kloet ER, Vreugdenhil E, Oitzl MS, Joels M. Brain corticosteroid receptor balance in health and disease. Endocrine Revs. 1998; 19:269–301. [PubMed: 9626555]

Duval F, Mokrani MC, Lopera FG, Diep TS, Rabia H, Fattah S. Thyroid axis activity and suicidal behavior in depressed patients. Psychoneuroendocrinology. 2010; 35:1045–1054. [PubMed: 20129737]

Furuya F, Lu C, Guigon CJ, Cheng SY. Nongenomic activation of phosphatidylinositol 3-kinase signaling by thyroid hormone receptors. Steroids. 2009; 74:628–634. [PubMed: 19014961]

Galton VA. Thyroid hormone receptors and iodothyronine deiodinases in the developing Mexican axolotl, *Ambystoma mexicanum*. Gen Comp Endocrinol. 1991; 85:62–70. [PubMed: 1563619]

Gussekloo J, Van Exel G, De Craen AJ, Meinders AE, Frolich M, Westendorp RG. Thyroid status, disability and cognitive function, and survival in old age. J Am Med Assoc. 2004; 292:2591–2599.

Irizarry RA, Hobbs B, Collin F, Beazer-Barclay YD, Antonellis KJ, Scherf U, Speed TP. Exploration, normalization, and summaries of high density oligonucleotide array probe level data. Biostatistics. 2003; 4:249–264. [PubMed: 12925520]

Koibuchi N. The role of thyroid hormone on cerebellar development. Cerebellum. 2008; 7:530–533. [PubMed: 18923818]

Kong WM, Martin NM, Smith KL, Gardiner JV, Connoley IP, Stephens DA, Dhillo WS, Ghatei MA, Small CJ, Bloom SR. Triiodothyronine stimulates food intake via the hypothalamic ventromedial nucleus independent of changes in energy expenditure. Endocrinology. 2004; 145:5252–5258. [PubMed: 15297436]

Krassas GE, Poppe K, Glinoer D. Thyroid function and human reproductive health. Endocr Rev. 2010; 31:702–755. [PubMed: 20573783]

Kuhn ER, De Groef B, Van der Geyten S, Darras MV. Corticotropin-releasing hormone-mediated metamorphosis in the neotenic axolotl Ambystoma mexicanum: Synergisitic involvement of thyroxine and corticoids on brain type II deiodinase. Gen Comp Endocr. 2005; 143:75–81. [PubMed: 15993107]

Kuhn, ER.; Jacobs, GFM. Metamorphosis. In: Armstrong, B.; Malacinski, GM., editors. Developmental Biology of the Axolotl. Oxford University Press; New York: 1989. p. 187-194.

Leggio L, Ferrulli A, Cardone S, Malandrino N, Mirijello A, D'Angelo C, Vonghia L, Miceli A, Capristo E, Kenna GA, Gasbarrini G, Swift RM, Addolorato G. Relationship between the hypothalamic-pituitary-thyroid axis and alcohol craving in alcohol-dependent patients: a longitudinal study. Alcohol Clin Exp Res. 2008; 32:2047–2053. [PubMed: 18828809]

Monaghan JR, Walker JA, Page RB, Putta S, Beachy CK, Voss SR. Early gene expression during natural spinal cord regeneration in the salamander *Ambystoma mexicanum*. J Neurochem. 2007; 101:27–40. [PubMed: 17241119]

Monaghan JR, Epp LG, Putta S, Page RB, Walker JA, Beachy CK, Zhu W, Pao GM, Verma IM, Hunter T, Bryant SV, Gardiner DM, Harkins TT, Voss SR. Microarray and cDNA sequence analysis of transcription during nerve dependent limb regeneration. BMC Biology. 2009; 7:1. [PubMed: 19144100]

Norman MF, Carr JA, Norris DO. Adenohypophysial-thyroid activity of the tiger salamander, Ambystoma tigrinum, as a function of metamorphosis and captivity. J Exp Zool. 1987; 242:55–66. [PubMed: 3598513]

Ooka H, Shinkai T. Effects of hyperthyroidism on the life span of the rat. Mech Aging Dev. 1986; 33:275–282. [PubMed: 3713266]

Oppenheimer JH, Schwartz HL, Surks MI. Tissue differences in the concentration of triiodothyronine nuclear binding sites in the rat: liver, kidney, pituitary, heart, brain, spleen, and testis. Endocrinology. 1974; 95:897–903. [PubMed: 4369384]

Page RB, Monaghan JR, Samuels AK, Smith JJ, Beachy CK, Voss SR. Microarray analysis identifies keratin loci as sensitive biomarkers for thyroid hormone disruption in the salamander *Ambystoma mexicanum*. Comp Biochem Physiol C Toxicol Pharmacol. 2006; 145:15–27. [PubMed: 16926121]

Page RB, Boley MA, Smith JJ, Putta S, Voss SR. Microarray analysis of a salamander hopeful monster reveals transcriptional signatures of paedomorphic brain development. BMC Evol Biol. 2010; 10:199. [PubMed: 20584293]

Page RB, Voss SR, Samuels AK, Smith JJ, Putta S, Beachy CK. Effect of thyroid hormone concentration on the transcriptional response underlying induced metamorphosis in the Mexican axolotl (*Ambystoma*). BMC Genomics. 2008; 9:78. [PubMed: 18267027]

Page, RB.; Voss, SR. Induction of metamorphosis in axolotls (Ambystoma mexicanum). Cold Spring Harbor Protocols; 2009.

Patel J, Landers K, Li H, Mortimer RH, Richard K. Thyroid hormones and fetal neurological development. Journal of Endocrinology. 2011 Jan 6. Epub ahead of print.

Pihlajamäki J, Boes T, Kim EY, Dearie F, Kim BW, Schroeder J, Mun E, Nasser I, Park PJ, Bianco AC, Goldfine AB, Patti ME. Thyroid hormone-related regulation of gene expression in human fatty liver. J Clin Endocrinol Metab. 2009; 94:3521–3529. [PubMed: 19549744]

Rosenkilde P, Ussing AP. What mechanisms control neoteny and regulate induced metamorphosis in urodeles? Int J Dev Biol. 1996; 40:665–673. [PubMed: 8877439]

Royland JE, Parker JS, Gilbert ME. A genomic analysis of subclinical hypothyroidism in hippocampus and neocortex of the developing rat brain. J Neuroendocrinol. 2008; 20:1319–338. [PubMed: 19094080]

Samuels HH, Tsai JS, Casanova J. Thyroid hormone action: in vitro demonstration of putative receptors in isolated nuclei and soluble nuclear extracts. Science. 1974; 184:1188–1191. [PubMed: 4364362]

Sanabra C, Mengod G. Neuroanatomical distribution and neurochemical characterization of cells expressing adenylyl cyclase isoforms in mouse and rat brain. J Chem Neuroanat. 2011; 41:43–54. [PubMed: 21094251]

Sap J, Munoz A, Damm K, Goldberg Y, Ghysdael J, Leutz A, Beug H, Vennstrom B. The c-erb-A protein is a high-affinity receptor for thyroid hormone. Nature. 1986; 324:635–640. [PubMed: 2879242]

Shaffer HB, Voss SR. Phylogenetic and mechanistic analysis of a developmentally integrated character complex: alternate life history modes in ambystomatid salamanders. Am Zool. 1996; 36:24–35.

Shi, YB. Amphibian Metamorphosis: From Morphology to Molecular Biology. Wiley-Liss Press; New York: 2000.

Shi ZX, Levy A, Lightman SL. Thyroid hormone-mediated regulation of corticotropin-releasing hormone messenger ribonucleic acid in the rat. Endocrinology. 1994; 134:1577–1580. [PubMed: 8119200]

Smith JJ, Putta S, Walker JA, Kump DK, Samuels AK, Monaghan JR, Weisrock DW, Staben C, Voss SR. Sal-site: integrating new and existing ambystomatid research and informational resources. BMC Genomics. 2005; 6:181. [PubMed: 16359543]

Tata JR. Gene expression during metamorphosis: an ideal model for post-embryonic development. Bioessays. 1993; 15:239–248. [PubMed: 8517853]

Tata JR. Amphibian metamorphosis as a model for the developmental actions of thyroid hormone. Mol Cell Endocrinol. 2006; 246:10–20. [PubMed: 16413959]

Thomas PD, Campbell MJ, Kejariwal A, Mi H, Karlak B, Daverman R, Diemer K, Muruganujan A, Narechania A. PANTHER: a library of protein families and subfamilies indexed by function. Genome Res. 2003; 13:2129–2141. [PubMed: 12952881]

Voss SR, Smith JJ. Evolution of salamander life cycles: a major-effect quantitative trait locus contributes to discrete and continuous variation for metamorphic timing. Genetics. 2005; 170:275–281. [PubMed: 15781701]

Weinberger C, Thompson CC, Ong ES, Lebo R, Gruol DJ, Evans RM. The c-erb-A gene encodes a thyroid hormone receptor. Nature. 1986; 324:641–646. [PubMed: 2879243]

Wong KK, Ng SY, Lee LT, Ng HK, Chow BK. Orexins and their receptors from fish to mammals: A comparative approach. Gen Comp Endocrinol. 2011; 171:134–140.

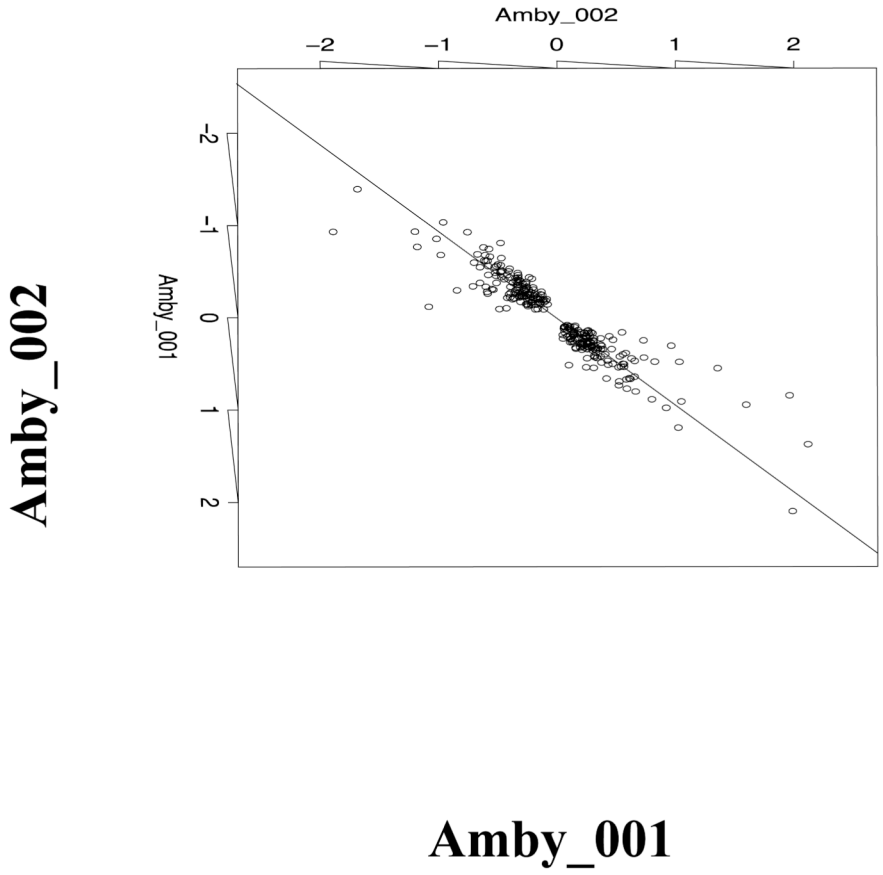

Figure 1.
Plot showing the D0-D18 difference in mean expression calculated for 281 probe sets identified at $p < 0.1$ from Amby_001 and Amby_002. The Spearman correlation is $r_s = 0.94$ and the regression line is $y = -0.014 + 1.062 \times$.

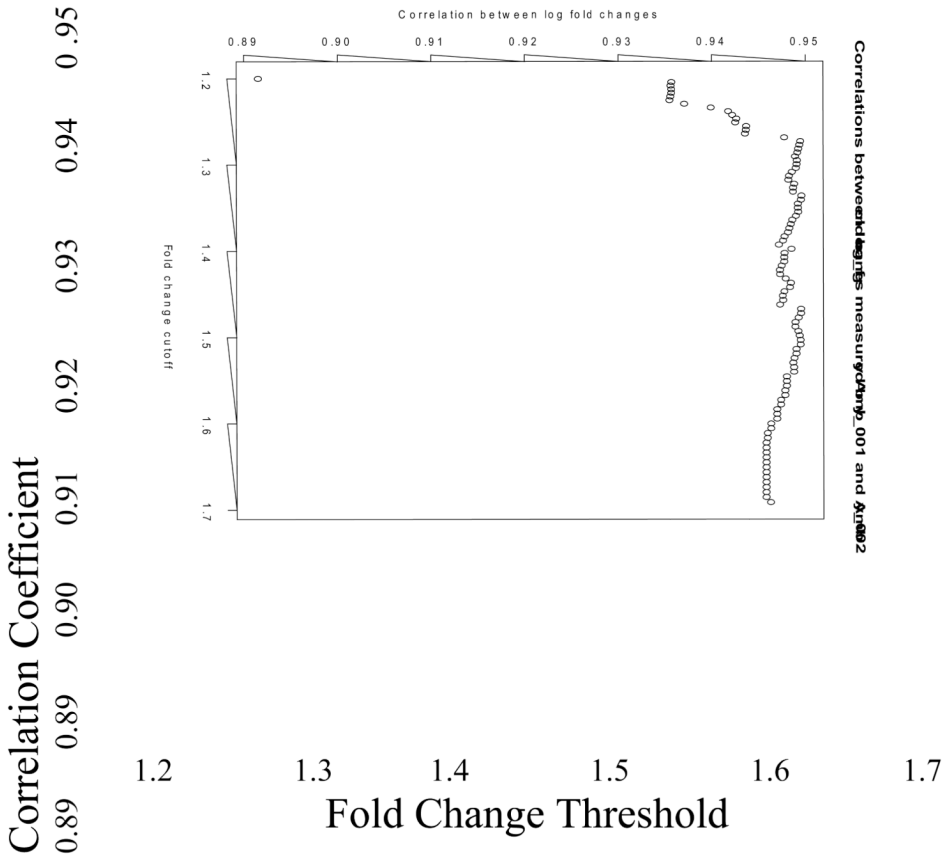

Figure 2.

Spearman correlation coefficients were calculated for groups of comparable probe sets between Amby_001 and Amby_002. The groups were created from the complete list of 2601 comparable probe sets using fold change as a criterion.

Table 1

454 DNA sequence reads that were generated for each cDNA brain library

	454_D0	454_D8	454_D18	Totals
Total Reads	645415	651424	769018	2065857
Filtered	43664	51904	46150	141718
mtRNA/rRNA	6935	15288	23376	45599
Final Reads	594816	584232	696684	1875732

Table 2

Annotation of genes discovered by 454 DNA sequencing to Panther biological processes with > 95 genes.

Panther Biological Process	# Genes
metabolic process	2457
primary metabolic process	2374
cellular process	2110
cell communication	1607
signal transduction	1520
nucleobase, nucleoside, nucleotide and nucleic acid	1174
transport	1016
developmental process	994
protein metabolic process	965
system process	922
cell surface receptor linked signal transduction	851
neurological system process	836
immune system process	778
system development	682
cell cycle	584
intracellular signaling cascade	545
protein transport	535
intracellular protein transport	535
ectoderm development	529
cell-cell signaling	521
response to stimulus	502
mesoderm development	497
nervous system development	488
cell adhesion	467
cellular component organization	454
vesicle-mediated transport	403
lipid metabolic process	369
cellular component morphogenesis	366
anatomical structure morphogenesis	366

Panther Biological Process	# Genes
cell motion	350
ion transport	336
reproduction	314
cell-cell adhesion	308
apoptosis	301
sensory perception	300
synaptic transmission	292
carbohydrate metabolic process	291
gamete generation	286
cation transport	282
endocytosis	201
mitosis	200
embryonic development	189
visual perception	186
muscle contraction	179
muscle organ development	171
immune response	166
response to stress	165
angiogenesis	164
skeletal system development	160
exocytosis	145
spermatogenesis	144
neurotransmitter secretion	144
heart development	133
cellular amino acid and derivative metabolic process	126
response to external stimulus	125
blood coagulation	125
pattern specification process	122
female gamete generation	116
cellular defense response	113
induction of apoptosis	107

Panther Biological Process	# Genes
blood circulation	98
negative regulation of apoptosis	95

Table 3

Annotation of genes discovered by 454 DNA sequencing to Panther biological pathways with > 10 genes.

Panther Pathway	# Genes
Wnt signaling	119
Inflammation mediated by chemokine and cytokine	81
Angiogenesis	77
Heterotrimeric G-protein signaling -Gi, Gs	71
Heterotrimeric G-protein signaling -Gq, Go	60
Cadherin signaling	59
PDGF signaling	53
Huntington disease	51
EGF receptor signaling	49
Metabotropic glutamate receptor group III	47
Apoptosis signaling	43
TGF-beta signaling	42
Interleukin signaling	42
Integrin signalling	42
Endothelin signaling	41
FGF signaling	40
Nicotinic acetylcholine receptor signaling	39
Alzheimer disease-presenilin	38
Ionotropic glutamate receptor	38
p53	33
Muscarinic acetylcholine receptor 1 and 3 signaling	33
Thyrotropin-releasing hormone receptor signaling	33
VEGF signaling	32
5HT2 type receptor mediated signaling	32
Parkinson disease	31
PI3 kinase	31
Insulin/IGF -protein kinase B signaling cascade	30
T cell activation	29
Muscarinic acetylcholine receptor 2 and 4 signaling	29

Panther Pathway	# Genes
Synaptic_vesicle_trafficking	27
Oxytocin receptor mediated signaling	27
Oxidative stress response	26
Alzheimer disease-amyloid secretase	25
Metabotropic glutamate receptor group II	24
Blood coagulation	23
Ras	22
B cell activation	22
Metabotropic glutamate receptor group I	20
Toll receptor signaling	19
Histamine H1 receptor mediated signaling	19
5HT1 type receptor mediated signaling	19
Alpha adrenergic receptor signaling	18
Adrenaline and noradrenaline biosynthesis	17
GABA-B_receptor_II_signaling	17
Beta2 adrenergic receptor signaling	17
Betal adrenergic receptor signaling	17
p53 feedback loops 2	16
Cytoskeletal regulation by Rho GTPase	16
Transcription regulation by bZIP transcription factor	15
Notch signaling	15
5HT4 type receptor mediated signaling	15
Axon guidance mediated by semaphorins	14
Heterotrimeric G-protein signaling -rod outer segment	14
Axon guidance mediated by netrin	13
Insulin/IGF -mitogen activated protein kinase kinase/M	12
Hypoxia response via HIF activation	12
Cortocotropin releasing factor receptor signaling	12
De novo purine biosynthesis	11
5HT3 type receptor mediated signaling	11
Hedgehog signaling	10

Panther Pathway	# Genes
General transcription regulation	10
Beta3 adrenergic receptor signaling	10

Table 4

Annotation of 211 significantly differentially expressed genes with Panther biological process terms. No terms were identified as significant for DN D0-D18. UP = genes that increased in abundance; DN = genes that decreased in abundance.

Biological Process Term	All Genes (N=211)	UP D0-D8 (N=71)	DN D0-D8 (N=40)	UP D8-D18 (N=85)	DN D8-D18 (N=71)	UP D0-D18 (N=30)
metabolic process	122				45	
primary metabolic process	116				42	
system process	38					
response to stimulus	30				12	
lipid metabolic process	27			11	10	
response to stress	12					
blood circulation	9				4	
chromosome segregation	8	4			5	
coenzyme metabolic process	6				3	
macrophage activation	6					
regulation of liquid surface tension	3				2	
neurological system process				16		
cell cycle		14				
mitosis		8				
vitamin metabolic process				3		
vitamin biosynthetic process				2		
anion transport			2			
acyl-CoA metabolic process					2	
oxygen metabolic process					2	
response to toxin						2
segment specification					3	
sulfur metabolic process					3	

Table 5

List of D0-D8 up-regulated genes that annotated to the neurological system process ontology term.

Gene Symbol	Neurological Process
PRKX	Serine/threonine-protein kinase PRKX
RASL11A	Ras-like protein family member 11A
EHD3	EH domain-containing protein 3
RPE65	Retinal pigment epithelium-specific 65 kDa protein
HCRTR2	Orexin receptor type 2
MAPKAP3	MAP kinase-activated protein kinase 3
HTR5A	5-hydroxytryptamine receptor 5A
MARS	Methionyl-tRNA synthetase, cytoplasmic
PTH2	Peptidyl-tRNA hydrolase 2, mitochondrial
ADORA1	Adenosine receptor A1
TULP3	Tubby-related protein 3
MARS	Src-like-adapter 2
NR3C2	Mineralocorticoid receptor
KCNJ3	G protein-activated inward rectifier potassium channel
ILF2	Interleukin enhancer-binding factor 2
NLGN4X	Neuroligin-4, X-linked